Network structure of $0.7SiO_2$–$0.3Na_2O$ glass from neutron and x-ray diffraction and RMC modelling

2007 J. Phys.: Condens. Matter 19 335209

(http://iopscience.iop.org/0953-8984/19/33/335209)

IOP PUBLISHING JOURNAL OF PHYSICS: CONDENSED MATTER

J. Phys.: Condens. Matter **19** (2007) 335209 (11pp) doi:10.1088/0953-8984/19/33/335209

Network structure of $0.7SiO_2$–$0.3Na_2O$ glass from neutron and x-ray diffraction and RMC modelling

M Fábián[1], P Jóvári[1], E Sváb[1], Gy Mészáros[1], T Proffen[2] and E Veress[3]

[1] Research Institute for Solid State Physics and Optics, H-1525 Budapest, POB 49, Hungary
[2] Los Alamos National Laboratory, Lujan Neutron Scattering Ctr, Los Alamos, NM 87545, USA
[3] Babeş-Bolyai University, Faculty of Chemistry, 11 Arany János Street, RO-3400 Cluj, Romania

E-mail: fabian@szfki.hu, jovari@sunserv.kfki.hu and svab@szfki.hu

Received 12 February 2007
Published 4 July 2007
Online at stacks.iop.org/JPhysCM/19/335209

Abstract

The structure of $0.7SiO_2$–$0.3Na_2O$ glass was investigated by means of neutron and high-energy x-ray diffraction. The maximum momentum transfer was 35 and 23.5 $Å^{-1}$ for the two experiments. The two datasets were modelled simultaneously by the reverse Monte Carlo simulation technique. By using reasonable constraints it was possible to separate the six partial pair correlation functions. Nearest neighbour distances, coordination numbers and bond angle distributions have been revealed. It was found that 63% of the O atoms are in the bridging position. The Na–O distance is 2.29 Å and the coordination number is 2.5. The Na–Na nearest neighbour distance is 2.6 Å, a value significantly smaller than previously reported. Neighbouring sodium ions tend to be located at the same oxygen atom. The average Si–O ring size is 7.6.

1. Introduction

Due to their diverse practical applications and fundamental scientific importance, alkali silicate glasses belong to the most intensely investigated disordered systems. They play a key role in optical technology and different chemical processes and more recently their multicomponent forms are candidates for high level nuclear waste storage. Physical and chemical properties of alkali silicates have been investigated by a wide range of experimental methods such as differential thermal analysis [1], photoelasticity [2] and transmission electron microscopy [3].

The structure of alkali silicates is investigated by a number of research groups. Besides experimental studies with neutron and x-ray diffraction [4–11], molecular dynamics [12–17], RMC simulations [8, 10, 11, 18], EXAFS [19, 20], NMR [21–24] and Raman scattering [8, 11, 23, 24] have also been applied to the study of these systems.

Though the above studies gave valuable information on alkali silicates there are still important problems unresolved in this field. For example, our knowledge about the coordination environment of the Na atoms is fairly limited.

In this paper we present a structural study of $0.7SiO_2$–$0.3Na_2O$ glass carried out by neutron diffraction (ND) and high energy x-ray diffraction (XRD). While neutron diffraction is often more sensitive to the scattering of light atoms, x-ray diffraction sees mostly the heavier elements. The combination of these two techniques is therefore very promising—especially if we take into account the weak contrast of the coherent neutron scattering amplitudes of available isotopes. The two measurements were modelled simultaneously by the reverse Monte Carlo technique, which gives a suitable framework for generating large 3D models compatible both with experimental results and *a priori* knowledge. The final aim of our study is the separation of the six partial pair correlation functions by modelling the experimental neutron and x-ray structure factors measured over an extended momentum transfer range. Besides this, we will also discuss the topology of the atomic configurations obtained by the modelling procedure.

2. Experimental details

2.1. Sample preparation

The sample was synthesized by melting 50 g quantity of previously homogenized mixture of dry SiO_2 and Na_2CO_3 powders (both p.a. grade, Reactivul, Bucuresti) in a platinum crucible. The melted mixture was kept at 1500 °C for 2 h, during which the melt was periodically homogenized by mechanical stirring. Thereafter, the melt was cooled to the pouring temperature, 1450 °C, and kept there for 30 min. The melt was quenched by pouring it on a stainless steel plate. Powder samples were prepared by powder milling of the quenched glasses in an agate mill.

2.2. Diffraction experiments

Neutron diffraction measurements were performed at the 10 MW research reactor of the Budapest Neutron Centre (BNC) and at the pulsed neutron source of the Los Alamos Neutron Science Center (LANSCE). Cylindrical vanadium sample holders of 8 and 10 mm diameter for the two experiments, respectively, were filled with the powder specimens of about 3–4 g each. The BNC measurement was carried out using the 'PSD' neutron powder diffractometer [25, 26]. The wavelength of radiation was $\lambda_0 = 1.07$ Å, and the scattered intensity was measured over the momentum transfer range $Q = 0.95$–10 Å^{-1}. The LANSCE measurement was performed at the 'NPDF' time-of-flight total scattering powder diffractometer [27]. The neutron wavelength varied from 0.17 to 4.2 Å, covering a momentum transfer range $Q = 1.5$–50 Å^{-1}. At low Q-values, around the first peak of the structure factor, $S(Q)$, the counting rate proved to be rather poor. This problem was solved by combining the data measured by the 'PSD' and 'NPDF' instruments. The structure factors were evaluated from the raw experimental data independently for the two types of measurements, using the programme packages available at the two facilities. The agreement of the $S(Q)$ data obtained from the 'PSD' and 'NPDF' measurements was within 5% in the overlapping Q-range. The $S(Q)$ patterns were combined by normalizing the 'PSD' data to the 'NPDF' in the 4–8 Å^{-1} interval by the least square method, and the average values of the two spectra were used for further data treatment. For $Q < 4$ Å^{-1} the 'PSD' data and for $Q > 8$ Å^{-1} the 'NPDF' data were used. The ND structure factor was obtained up to 35 Å^{-1}.

The x-ray diffraction measurement was carried out at the BW5 experimental station [28] at HASYLAB, DESY. A quartz capillary of 2 mm diameter (wall thickness of ∼0.02 mm) was filled with the powdered sample. The energy of the radiation was 99.8 keV. Raw data

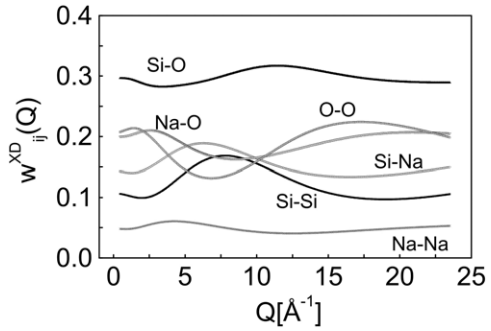

Figure 1. The Q-dependent x-ray weighting factors, $w_{ij}^{\mathrm{XD}}(Q)$, for the six different atom pairs of $0.7SiO_2$–$0.3Na_2O$ glass.

Table 1. Neutron and x-ray weighting factors, $w_{ij}(Q)$ (%) for the $0.7SiO_2$–$0.3Na_2O$ glass.

	Si–O	O–O	Si–Si	Na–O	Si–Na	Na–Na
w_{ij}^{ND}	25.7	43.5	3.8	19.2	5.7	2.1
w_{ij}^{XD} ($Q = 0.8$ Å^{-1})	29.6	20.8	10.6	19.9	14.3	4.8

were corrected for detector dead time, background, polarization, absorption and variations in detector solid angle. The XRD structure factor was obtained up to 23.5 Å^{-1}.

The x-ray scattering amplitude for the various elements is Q dependent, and for each atom in a somewhat different way, therefore the weighting factors of the partial structure factors [29], $w_{ij}^{\mathrm{XD}}(Q)$ are also Q dependent, as illustrated in figure 1. In order to compare the corresponding weighting factors for the two types of radiation, table 1 includes the Q-independent w_{ij}^{ND} together with a characteristic value for w_{ij}^{XD} at $Q = 0.8$ Å^{-1}.

2.3. The reverse Monte Carlo method

The reverse Monte Carlo (RMC) method has been shown to be a useful tool to investigate various structural aspects of disordered materials. In the RMC simulation technique the atoms of an initial configuration are moved around in order to reproduce the measured data within the experimental uncertainties [30]. Compared with the traditional data evaluation techniques based on the direct Fourier transform of experimental structure factors, RMC has several advantages, two of which will be extensively used in the present work. First, diffraction datasets recorded over different experimental ranges can be combined in one model. Second, our *a priori* knowledge on the system investigated can be incorporated in the model configuration by using e.g. coordination number constraints or minimum interatomic distances.

The simulation box contained 6000 atoms. The density was 0.071 atoms Å^{-3} [16]. The minimum interatomic distances were 1.4, 2.1, 2.4 and 2.9 Å, for Si–O, Na–O, O–O and Si–Si pairs, respectively, in accordance with the expected first neighbour distance known fairly well from the literature. These values were the same in all simulation runs. Several different Si–Na and Na–Na cut-off distances were tried between 2.5 and 3.1 Å. It was found that partial pair correlation functions showed artificially sharp features if the Si–Na and Na–Na cut-off distances were higher than 2.8 Å. Therefore, further simulations were carried out

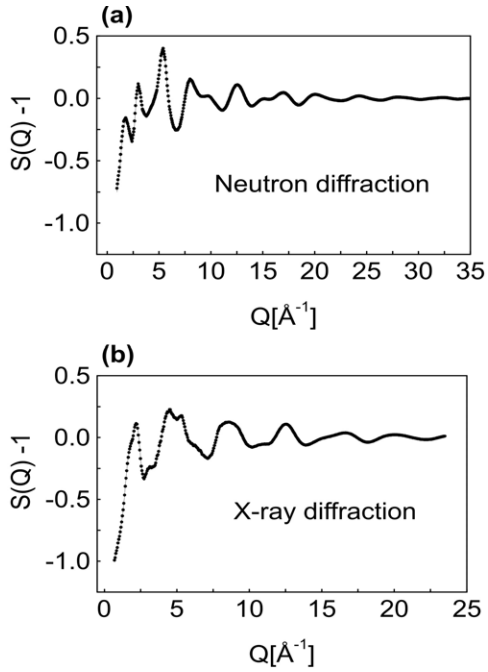

Figure 2. The total structure factors of $0.7SiO_2$–$0.3Na_2O$ glass. Experimental data (circles) and simultaneous RMC fit (solid lines) for model B: (a) neutron diffraction and (b) x-ray diffraction.

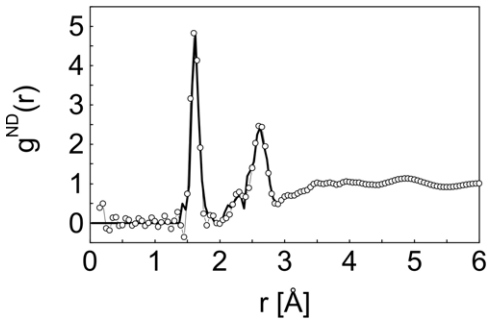

Figure 3. Comparison of the experimental (circles) and the RMC (solid line) neutron total pair correlation function of $0.7SiO_2$–$0.3Na_2O$ glass.

only with the following Na–Na/Si–Na cut-off distances: 2.5 and 2.5 Å (model A) and 2.5 and 2.8 Å (model B). The initial configuration was prepared from a completely random distribution of atoms in two main steps. First a hard sphere Monte Carlo simulation was carried out to remove overlapping atoms. After this the following coordination number constraints were applied: (i) each Si was forced to have exactly four O neighbours between 1.4 and 1.9 Å, (ii) O atoms were forced to have at most two Si neighbours between the same limits.

The above constraints were fulfilled for at least 95% of the corresponding atoms. The final model $S(Q)$s matched very well the experimental structure factors, as shown in figure 2, obtained from the simultaneous fit of neutron and x-ray diffraction data. The quality of the agreement is also illustrated in figure 3 for the neutron total pair correlation function, $g^{\mathrm{ND}}(r)$,

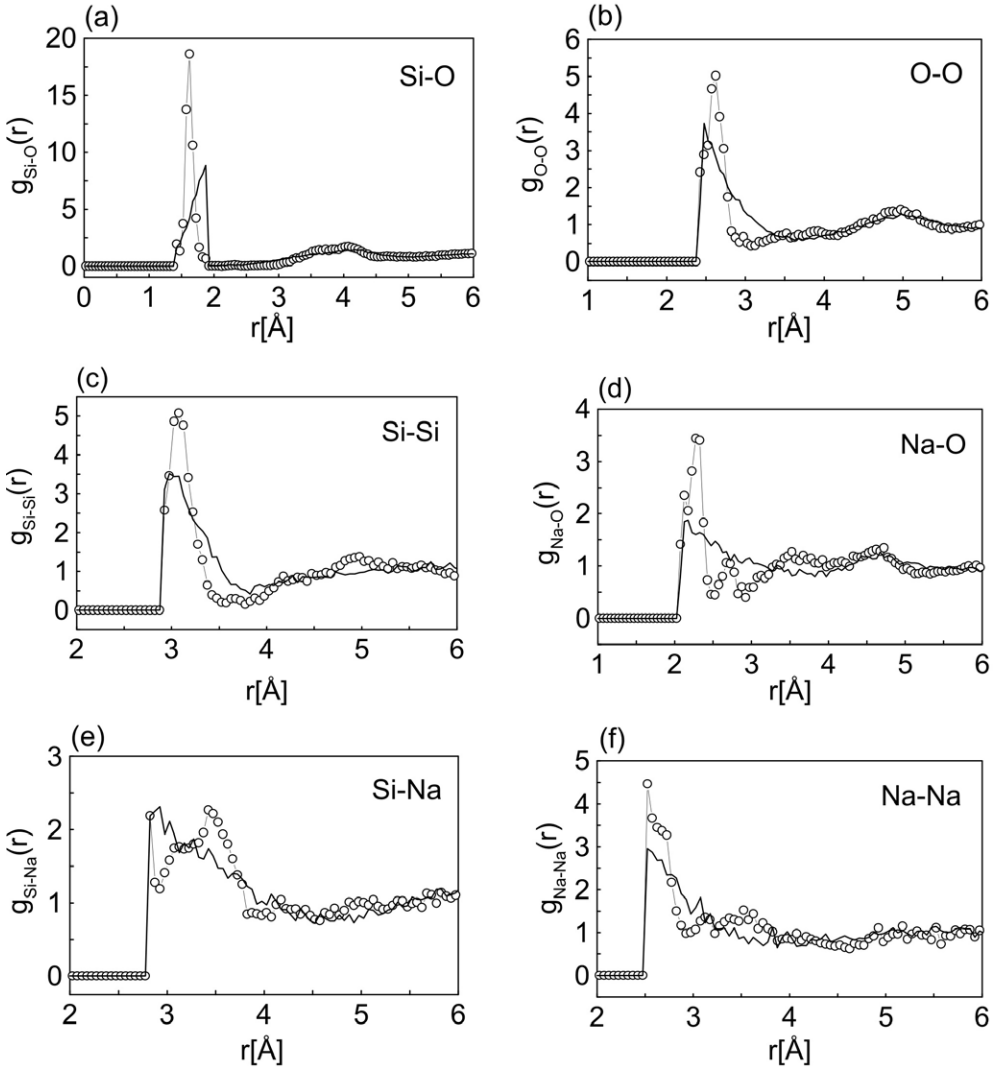

Figure 4. The partial pair distribution functions obtained by the simultaneous RMC fit of the two measurements (open circle: model B) and calculated from the initial configuration (solid line): (a) Si–O pair, (b) O–O pair, (c) Si–Si pair, (d) Na–O pair, (e) Si–Na pair, (f) Na–Na pair.

by comparing the experimental one calculated by Fourier transformation from the $S(Q)$ data with that obtained by the RMC modelling.

3. Results and discussion

Glassy silicates possess a well defined short range order without long range correlations characteristic of crystalline systems. The use of constraints in RMC makes it possible to mimic the short range order of covalent glasses in a simple and computationally efficient way. This is illustrated by figures 4 and 5, where we compare the partial pair correlation functions, $g_{ij}(r)$, and partial structure factors, $S_{ij}(Q)$, obtained by simulating the measurements and

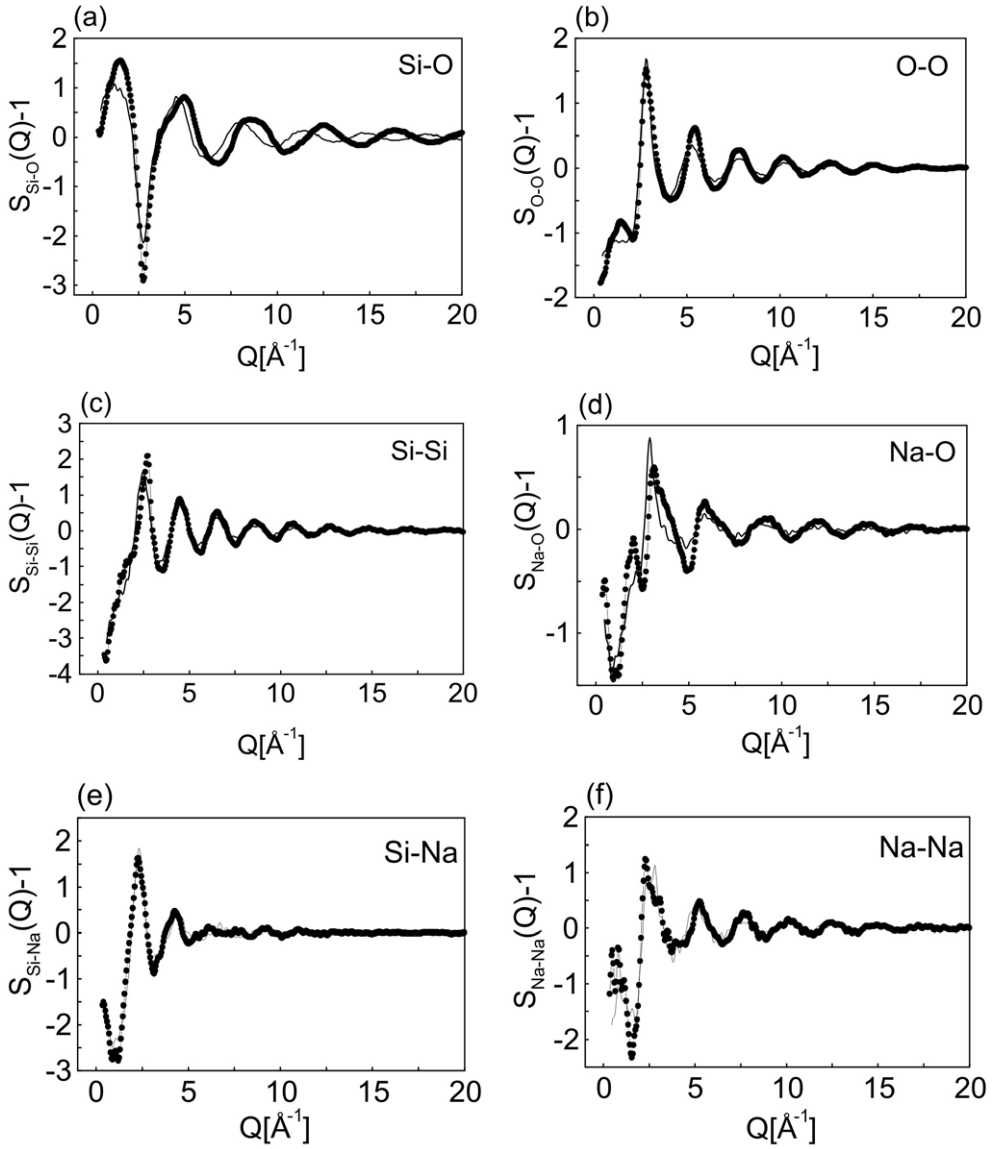

Figure 5. The partial structure factors obtained by the simultaneous RMC fit of the two measurements (circle: model B) and calculated from the initial configuration (solid line): (a) Si–O pair, (b) O–O pair, (c) Si–Si pair, (d) Na–O pair, (e) Si–Na pair, (f) Na–Na pair.

calculated from the initial model, respectively. It can be seen that as a result of the rather loose constraints applied to the Si–O coordination the Si–Si and O–O partial pair correlation functions are qualitatively reproduced by the initial configuration. The corresponding partial structure factors also show a qualitative agreement.

The functions $g_{SiO}(r)$, $g_{OO}(r)$, $g_{SiSi}(r)$ and $g_{NaO}(r)$ obtained from models A and B (and from other models not discussed here) are practically identical, whereas $g_{SiNa}(r)$ and $g_{NaNa}(r)$ calculated by the two different sets of constraints are rather different; they are compared in figure 6. In model A both Si–Na and Na–Na minimum distances were set to 2.5 Å. The

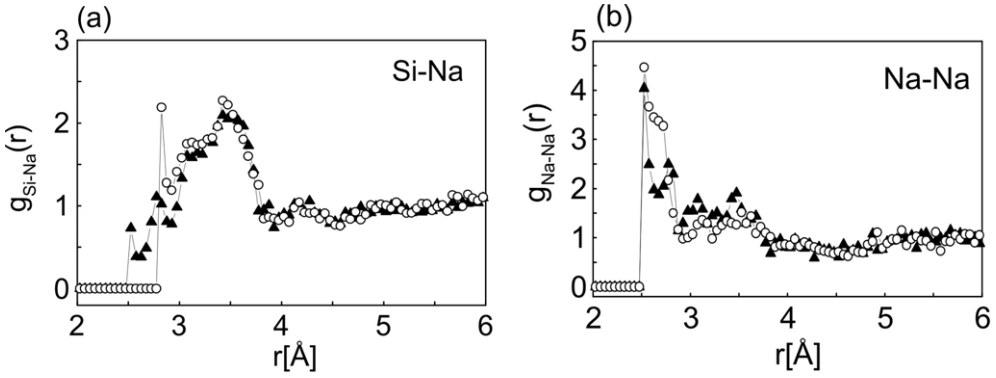

Figure 6. The model dependence of Si–Na (a) and Na–Na (b) partial pair distribution functions (triangle, model A; open circle, model B).

first peak of $g_{\mathrm{SiNa}}(r)$ is rather broad, with a maximum at about 3.5 Å. The $g_{\mathrm{NaNa}}(r)$ contains oscillations up to 3.9 Å. In model B we increased the Si–Na cut-off distance to 2.8 Å. As a result the $g_{\mathrm{SiNa}}(r)$ is practically unchanged, with a maximum at about 3.5 Å, while the $g_{\mathrm{NaNa}}(r)$ contains a reasonable first peak at around 2.6 Å. From these findings we conclude that model B gives a reasonable result, and the forthcoming presentation is based on model B. The Na–Na coordination number calculated from this model is 1.5, thus a significant number of Na atoms have more than one Na neighbour. The Na–O–Na bond-angle distribution shows a pronounced peak at about 70° (figure 8), thus the peak of $g_{\mathrm{NaNa}}(r)$ at 2.6 Å is mostly due to Na–Na pairs that are in the vicinity of the *same* oxygen atom.

If the Si–Na and Na–Na cut-off distances are larger than 3 Å, then the missing peaks of $g_{\mathrm{NaNa}}(r)$ and/or $g_{\mathrm{SiNa}}(r)$ are compensated by shifting the first peak of $g_{\mathrm{SiSi}}(r)$ to smaller r values (e.g. 2.95 Å). Such a drastic and artificial change of the well defined (and well known) Si–Si distance clearly indicates that at least one of the Si–Na and Na–Na peaks should be located well below 3 Å. We have obtained that the Na–Na first neighbour distance is at 2.6 Å, in accordance with this expectation. However, this relatively short distance is considerably less than the corresponding values of 3.0–3.1 Å obtained from recent MD calculations (see [17] and references therein). On the other hand the 3.5 Å for Si–Na distance fairly well agrees with the 3.4 Å reported in [8, 17].

Due to the rather low weights of the Si–Na and Na–Na partial structure factors and the proximity of the pronounced O–O peaks, previous neutron diffraction studies focusing on the total pair correlation function could not give detailed information on $g_{\mathrm{NaNa}}(r)$ and $g_{\mathrm{SiNa}}(r)$. The combination of XRD and ND results and the use of a *model* based on our *a priori* knowledge help to circumvent both difficulties.

The interatomic distances and coordination numbers are listed in table 2. Due to the constraints applied the Si–O coordination number is close to 4.0. The average O–Si coordination number is 1.6. The O–Si coordination number distribution (figure 7) indicates that 63% of the oxygen atoms are in the bridging position (O_B—connected to two silicon atoms) while 34% of them are terminal (O_T—connected to one silicon atom). A small fraction of O atoms has no Si neighbour at all.

The first Na–O distance at 2.29 Å is well separated both from the Si–O covalent bond length (1.62 Å) and from the first O–O distance (2.62 Å). Furthermore, the weights of the Na–O partial structure factor are relatively large (∼0.19 in both experimental structure factors), therefore the Na–O distance and coordination number can also be determined with

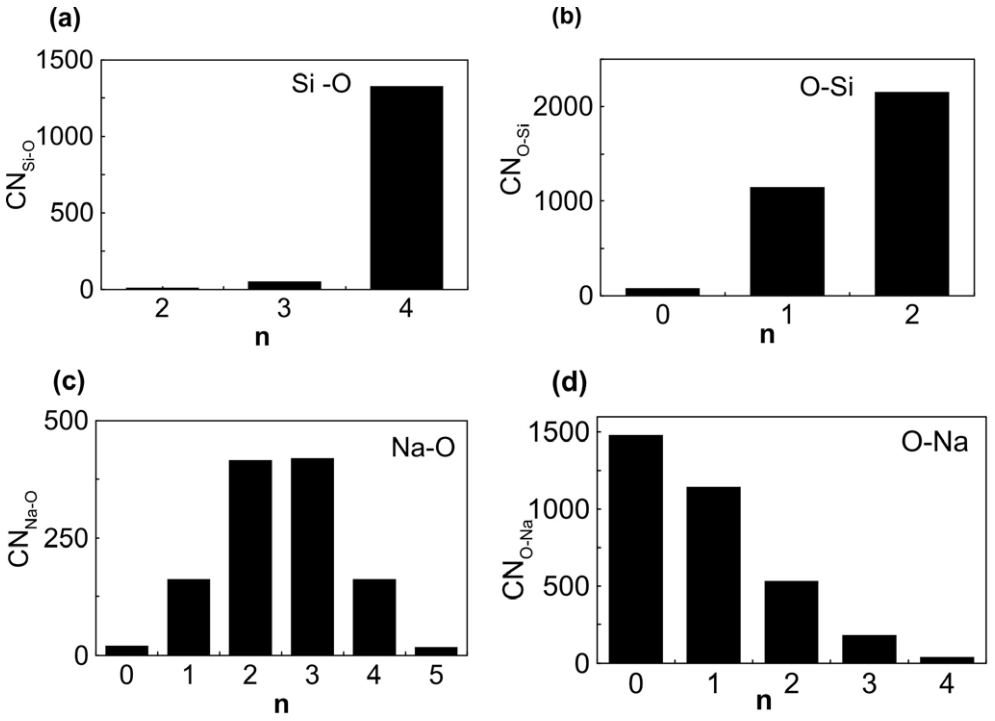

Figure 7. Coordination number distributions: (a) Si–O, (b) O–Si, (c) Na–O and (d) O–Na.

Table 2. The interatomic distances, r_{ij} (Å) and coordination numbers, CN_{ij}. The corresponding radii (Å) are indicated in brackets.

	r_{ij}	CN_{ij}
Si–O	1.62 ± 0.005	3.94 ± 0.005 (1.45–1.95)
O–O	2.62 ± 0.05	5.8 ± 0.2 (2.1–3.2)
Si–Si	3.05 ± 0.05	3.4 ± 0.5 (2.5–3.5)
Na–O	2.29 ± 0.05	2.5 ± 0.5 (2.05–2.45)
	2.7 ± 0.1	3.8 ± 0.5 (2.05–3.0)[a]
Si–Na	3.5 ± 0.1	4.6 ± 0.5 (2.1–3.9)
Na–Na	2.6 ± 0.1	1.5 ± 0.5 (2.5–2.9)
		3.8 ± 0.5 (2.5–3.8)[a]

[a] The coordination numbers are calculated up to an extended distance to make our results comparable with the data reported in [8, 17] and references therein.

a rather high accuracy. The first peak positions of $g_{SiO}(r)$, $g_{OO}(r)$, $g_{SiSi}(r)$ and $g_{NaO}(r)$ and the corresponding coordination numbers are rather stable and within reasonable limits are not sensitive to the choice of minimum interatomic distances. The average Na–O coordination number calculated up to 2.45 Å is 2.5. In [6, 8] the second Na–O peak at about 2.5 ± 0.2 Å was assigned to Na–O_B correlations. A detailed investigation of our configurations does not support this interpretation; however, as such fine details are not necessarily reconstructed by RMC, the separation of Na–O_T and Na–O_B peaks cannot be excluded on the basis of the present study.

Some bond-angle distributions are shown in figure 8. The peak of the Si–O–Si distribution is at 149° while the O–Si–O distribution is centred at 107°, very close to 109.5°, the ideal tetrahedral angle. The bond angle distribution is asymmetric with a tail at high angles affecting

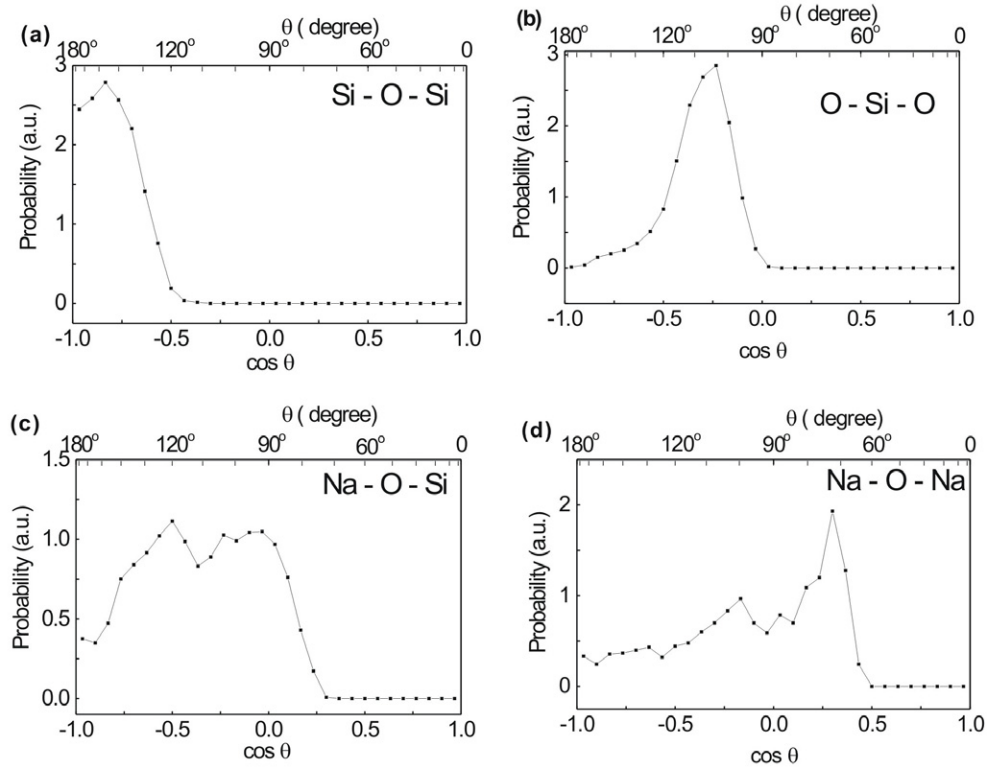

Figure 8. Bond-angle distributions: (a) Si–O–Si, (b) O–Si–O, (c) Na–O–Si and (d) Na–O–Na.

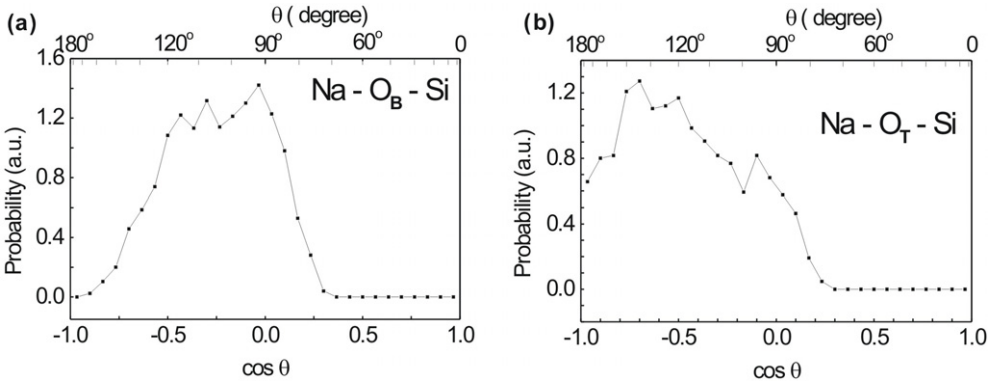

Figure 9. The bond-angle distributions for (a) Na–O_B–Si and (b) Na–O_T–Si.

roughly 5–10% of O–Si–O bonds. Test runs on SiO_2 with the same constraints on Si–O coordination yielded configurations with very similar O–Si–O bond-angle distribution. Thus the tail at high angles is a consequence of the distortion of SiO_4 tetrahedra allowed by the constraints applied. For the Na–O–Si bond angles we found that the Na–O_B–Si and Na–O_T–Si distributions are significantly different (figure 9). Due to the presence of a second Si neighbour the Na–O_B–Si bond-angle distribution is centred around 90°–120°, while the broad peak of

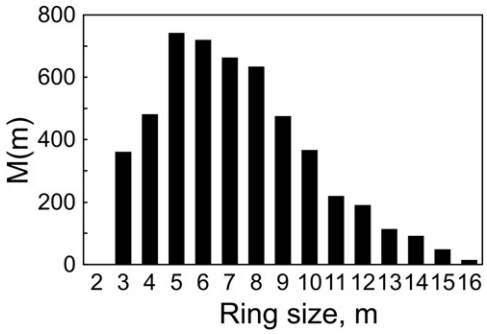

Figure 10. Ring size distribution in $0.7SiO_2$–$0.3Na_2O$.

the Na–O_T–Si distribution between 100° and 155° suggests a more open arrangement around terminal oxygen atoms.

The medium range structure of network glasses is usually characterized by the ring size distribution. For silica glass the ring size distribution extends from three- to ten-membered rings, with a maximum of about six-membered rings; see, e.g., [31]. The ring size distribution in Na silicates was investigated by Cormack and Du by molecular dynamics [17]. In their work the peak of the distribution was at seven-membered rings and the tail of the distribution extended to 25-membered rings. Besides this 'main' peak they had several other maxima at larger ring sizes (e.g. 10, 13, 16), which can be regarded as 'combinational peaks' obtained by merging two smaller rings. Figure 10 shows the ring size statistics—the number of m-membered rings, $M(m)$—calculated from the atomic configuration obtained by our RMC simulation. The distribution has a rather flat maximum for five- to eight-membered rings. Although the tail of the distribution extends to 16-membered rings, 90% of the rings contain ten or fewer Si atoms, resulting in an average of 7.6-membered rings. Though the actual shape of the distribution revealed by us is different from that reported in [17], the agreement of the peak positions is remarkable.

4. Conclusions

The structure of $0.7SiO_2$–$0.3Na_2O$ glass has been modelled by fitting neutron and x-ray diffraction measurements by the reverse Monte Carlo technique. It has been found that 63% of the O atoms are in the bridging position. The Na–O distance is 2.29 Å and the coordination number is 2.5. A detailed investigation of the atomic configurations obtained by RMC has shown that at least one of the Si–Na and Na–Na peaks should be located well below 3 Å. For the Na–Na nearest neighbour distance 2.6 Å was obtained, a value significantly smaller than previously reported. The Na–O–Na bond-angle distribution revealed that neighbouring sodium ions tend to be located at the same oxygen atom. The average ring size is 7.6 and the occurrence of larger rings ($m > 10$) is relatively low.

Acknowledgments

This study was supported by the Hungarian Research Grants OTKA T-042495, T-048580 and EC HPRI-RII3-CT-2003-505925. Our work has benefited from the use of NPDF at the Lujan Center at Los Alamos Neutron Science Center, funded by DOE Office of Basic Energy Sciences, and Los Alamos National Laboratory, funded by the Department of Energy under

contract W-7405-ENG-36. The upgrade of NPDF has been funded by NSF through grant DMR 00-76488.

References

[1] Avramov I, Vassilev Ts and Penkov I 2005 *J. Non-Cryst. Solids* **351** 472
[2] Donadio D, Bernasconi M and Tassone F 2004 *Phys. Rev.* B **70** 214205
[3] Prado M O, Campos A A Jr, Soares P C, Rodrigues A C M and Zanotto E D 2003 *J. Non-Cryst. Solids* **332** 166
[4] Misawa M, Price D L and Suzuki K 1980 *J. Non-Cryst. Solids* **37** 85
[5] Wright A C, Clare A G, Bachra B, Sinclair R N, Hannon A C and Vessal B 1991 *Trans. Am. Crystallogr. Assoc.* **27** 239
[6] Cormier L, Gaskell P H, Calas G and Soper A M 1998 *Phys. Rev.* B **58** 11322
[7] Cormier L, Ghaleb D, Delaye J M and Calas G 2000 *Phys. Rev.* B **61** 14495
[8] Zotov N and Keppler H 1998 *Phys. Chem. Minerals* **25** 259
[9] Schlenz H, Neuefeind J and Rings S 2003 *J. Phys.: Condens. Matter* **15** 4919
[10] Majérus O, Cormier L, Calas G and Beuneu B 2004 *Chem. Geol.* **213** 89
[11] Karlsson C, Zanghellini E, Swenson J, Roling B, Bowron D T and Börjesson L 2005 *Phys. Rev.* B **72** 064206
[12] Smith W, Greaves G N and Gillan M J 1995 *J. Chem. Phys.* **103** 3091
[13] Cormack A N and Cao Y 1997 *Modelling of Minerals and Silicated Materials* ed B Silvi and P Arco (Dordrecht: Kluwer)
[14] Oviedo J and Sanz J F 1998 *Phys. Rev.* B **58** 9047
[15] Horbach J, Kob W and Binder K 2001 *Chem. Geol.* **174** 87
[16] Yuan X and Cormack A N 2001 *J. Non-Cryst. Solids* **283** 69
[17] Du J and Cormack A N 2004 *J. Non-Cryst. Solids* **349** 66
Du J and Cormack A N 2005 *J. Non-Cryst. Solids* **351** 2263
[18] McGreevy R L and Zetterström P 2001 *J. Non-Cryst. Solids* **293** 297
[19] Henderson G S 1995 *J. Non-Cryst. Solids* **183** 43
[20] Greaves G N and Fontaine A 1981 *Nature* **293** 611
[21] Dupree R, Holland D, McMillan P W and Pettifer R F 1984 *J. Non-Cryst. Solids* **68** 399
[22] Stebbins J F 1988 *J. Non-Cryst. Solids* **106** 359
[23] Maekawa H, Maekawa T, Kawamura K and Yokokawa T 1991 *J. Non-Cryst. Solids* **127** 53
[24] Dean W M, Shiv K S and John A P 1983 *J. Non-Cryst. Solids* **58** 323
[25] Sváb E, Deák F and Mészáros Gy 1996 *Mater. Sci. Forum.* **228** 247
[26] http://www.bnc.hu/
[27] http://lansce.lanl.gov/lujan/instruments/NPDF
[28] Poulsen H, Neuefeind J, Neumann H B, Schneider J R and Zeidler M D 1995 *J. Non-Cryst. Solids* **188** 63
[29] Gruner S, Kaban I, Kleinhempel R, Hoyer W, Jóvári P and Delaplane R G 2005 *J. Non-Cryst. Solids* **351** 3490
[30] McGreevy R L and Pusztai L 1988 *Mol. Simul.* **1** 359
[31] Kohara S and Suzuya K 2005 *J. Phys.: Condens. Matter* **17** S77